

Therapeutic advantage of targeting lysosomal membrane integrity supported by lysophagy in malignant glioma

Yongwei Jing¹ | Masahiko Kobayashi¹ | Ha Thi Vu¹ | Atsuko Kasahara^{2,3} | Xi Chen¹ |
 Loc Thi Pham¹ | Kenta Kurayoshi¹ | Yuko Tadokoro^{1,3} | Masaya Ueno^{1,3} |
 Tomoki Todo⁴ | Mitsutoshi Nakada⁵  | Atsushi Hirao^{1,3} 

¹Division of Molecular Genetics, Cancer Research Institute, Kanazawa University, Kanazawa, Japan

²Institute for Frontier Science Initiative, Kanazawa University, Kanazawa, Japan

³WPI Nano Life Science Institute (WPI-Nano LSI), Kanazawa University, Kanazawa, Japan

⁴Division of Innovative Cancer Therapy, Institute of Medical Science, The University of Tokyo, Tokyo, Japan

⁵Department of Neurosurgery, Graduate School of Medical Science, Kanazawa University, Kanazawa, Japan

Correspondence

Atsushi Hirao, Division of Molecular Genetics, Cancer Research Institute, Kanazawa University, Kakuma-machi, Kanazawa 920-1192, Japan.
 Email: ahirao@staff.kanazawa-u.ac.jp

Funding information

This work was supported by a Grant-in-Aid for Scientific Research (A) (19H01033) (A.H.); a Grant-in-Aid for Scientific Research (C) (20K07566) (M.K.) from the Ministry of Education, Culture, Sports, Science, and Technology (MEXT) of Japan; and a Grant-in-Aid for Project for Cancer Research and Therapeutic Evolution (P-CREATE) (21cm0106104h0006) from the Japan Agency for Medical Research and Development (AMED) (A.H.).

Abstract

Lysosomes function as the digestive system of a cell and are involved in macromolecular recycling, vesicle trafficking, metabolic reprogramming, and progrowth signaling. Although quality control of lysosome biogenesis is thought to be a potential target for cancer therapy, practical strategies have not been established. Here, we show that lysosomal membrane integrity supported by lysophagy, a selective autophagy for damaged lysosomes, is a promising therapeutic target for glioblastoma (GBM). In this study, we found that ifenprodil, an FDA-approved drug with neuromodulatory activities, efficiently inhibited spheroid formation of patient-derived GBM cells in a combination with autophagy inhibition. Ifenprodil increased intracellular Ca^{2+} level, resulting in mitochondrial reactive oxygen species-mediated cytotoxicity. The ifenprodil-induced Ca^{2+} elevation was due to Ca^{2+} release from lysosomes, but not endoplasmic reticulum, associated with galectin-3 punctation as an indicator of lysosomal membrane damage. As the Ca^{2+} release was enhanced by ATG5 deficiency, autophagy protected against lysosomal membrane damage. By comparative analysis of 765 FDA-approved compounds, we identified another clinically available drug for central nervous system (CNS) diseases, amoxapine, in addition to ifenprodil. Both compounds promoted degradation of lysosomal membrane proteins, indicating a critical role of lysophagy in quality control of lysosomal membrane integrity. Importantly, a synergistic inhibitory effect of ifenprodil and chloroquine, a clinically available autophagy inhibitor, on spheroid formation was remarkable in GBM cells, but not in nontransformed neural progenitor cells. Finally, chloroquine dramatically enhanced effects of the compounds inducing lysosomal membrane damage in a patient-derived xenograft model. These data demonstrate a therapeutic advantage of targeting lysosomal membrane integrity in GBM.

Abbreviations: BBB, blood-brain barrier; CNS, central nervous system; CQ, chloroquine; DMSO, dimethyl sulfoxide; ER, endoplasmic reticulum; GBM, glioblastoma; LLOMe, L-leucyl-L-leucine methyl ester; ROS, reactive oxygen species.

This is an open access article under the terms of the [Creative Commons Attribution-NonCommercial-NoDerivs](https://creativecommons.org/licenses/by-nc-nd/4.0/) License, which permits use and distribution in any medium, provided the original work is properly cited, the use is non-commercial and no modifications or adaptations are made.

© 2022 The Authors. *Cancer Science* published by John Wiley & Sons Australia, Ltd on behalf of Japanese Cancer Association.

KEYWORDS

autophagy, calcium, glioblastoma, lysosomal membrane integrity, lysosomal membrane turnover

1 | INTRODUCTION

Autophagy is a conserved catabolic system that degrades cellular components and contributes to the maintenance of cellular functions.¹ Autophagy is induced at a high level in response to insults such as oxidative stress, infection, and starvation.² Therefore, it is a survival mechanism that maintains cellular homeostasis.¹ Accumulating evidence has revealed that autophagy is involved in various pathophysiological phenomena such as tumorigenesis and malignant progression.³ Autophagy plays roles in quality control of cellular functions in a nonselective or selective process.⁴ During starvation, cellular components are degraded to maintain nutrients in a nonselective manner, whereas selective autophagy is required to maintain the number and integrity of cellular organelles.⁵

A lysosome is an acidic membrane-bound organelle with more than 50 hydrolytic enzymes and serves as a cellular digestive center in which intra- and extracellular components are degraded by fusing with autophagosomes or endosomes for quality control of cellular components and to supply recycling materials.⁶ Degradation of damaged lysosomes is named lysophagy, a selective autophagy.⁷ Furthermore, a recent study has revealed a novel mechanism of lysophagy, in which lipidation of the autophagy protein LC3 on lysosomal membranes directly leads to the formation of intraluminal vesicles without autophagosomal formation.⁷ This study demonstrated that ATG5-dependent lysosomal membrane turnover, which is classified as microautophagy, is induced by metabolic stress or osmotic stress in lysosomes. Thus, lysophagy plays a critical role in the maintenance of healthy lysosomes as both macro- and microautophagy systems. However, the role of lysophagy in cancer therapy has not been elucidated.

Glioblastoma (GBM) is the most common central nervous system (CNS) tumor, which is a very aggressive, invasive, and destructive brain tumor characterized by high-grade astrocytic tumors.⁸ Despite recent trials using multimodality therapeutic approaches, the 5-year survival rate has remained extremely low.⁹ Therefore, development of innovative therapeutic approaches to overcome these challenges is needed. Because autophagy is reportedly required for gliomagenesis,¹⁰ chloroquine (CQ), an autophagy inhibitor, has been tested as a treatment for high-grade brain tumors. However, the results of clinical trials have not been encouraging.¹¹ Consistently, we have previously reported that ATG5 disruption does not change the phenotypes of GBM cells *in vitro* or *in vivo* and does not enhance the efficacy of temozolomide.¹² Instead, autophagy inhibition sensitizes GBM cells to the effects of chemical compounds, such as nigericin and salinomycin, which induce Ca²⁺ mobilization.¹² Therefore, we hypothesized that a novel therapeutic strategy in which calcium-mobilizing compounds are combined with autophagy inhibitors would be able to treat GBM patients. However, because there is no

information on blood-brain barrier (BBB) penetration by nigericin and salinomycin, which are not FDA-approved drugs, these compounds are not practical for clinical application. Therefore, further analyses are needed to pursue a more practical methodology.

In this study, we investigated the effects of FDA-approved drugs for treatment of CNS diseases to determine whether practical chemotherapy can be established. This drug-repurposing strategy is expected to reduce overall development costs and shorten development timelines. As a result, we identified ifenprodil and amoxapine, as compounds that efficiently suppress spheroid formation of patient-derived GBM cells with autophagy inhibition. Detailed analysis of the mechanism of these compounds revealed that lysosomal membrane integrity supported by lysophagy is a potent therapeutic target.

2 | MATERIALS AND METHODS

2.1 | Compounds

The following chemical compounds were used: ifenprodil (Selleck), MRT68921 (Selleck), bafilomycin A1 (Sigma Aldrich), thapsigargin (Sigma Aldrich), N-acetyl-L-cysteine (NAC, Sigma Aldrich), CQ (Sigma Aldrich), amoxapine (Wako), BAPTA (Dojindo), and L-leucyl-L-leucine methyl ester (LLOMe, Funakoshi).

2.2 | Cell lines and culture

Patient-derived GBM cell lines (TGS04, KGS03, KGS04, and KGS22) were used in this study.¹² Collection of human materials and related experimental protocols were approved by the Ethics Committees of Kanazawa University and The University of Tokyo. ATG5-knockout GBM cells were previously generated by the CRISPR-Cas9 system.¹² Human neural stem/progenitor cells (NSPCs) were purchased from Lonza. GBM and NSPCs were cultured in NSPC medium at 37°C in a humidified atmosphere with 5% CO₂ and 5% oxygen.¹² HEK 293T cells and 293GP cells were cultured in high-glucose DMEM (Thermo Fisher Scientific) with 10% FBS and penicillin/streptomycin at 37°C and 5% CO₂ in a humidified incubator.

2.3 | Constructs

pLAMP1-mGFP (Plasmid #34831),¹³ mCherry-Lysosome20 (Plasmid #55073), and pEGFP-hGal3 (Plasmid #73080)¹⁴ were purchased from Addgene. A DNA fragment of EGFP-hGal3 was amplified from the pEGFP-hGal3 by PCR and inserted into the pLJM1 lentivirus

vector digested with restriction enzymes *EcoRV* and *Sall* to construct pLJM1-EGFP-hGal3. A fragment was amplified from the pGP-CMV-GCaMP6s (Plasmid #40753, Addgene)¹⁵ by PCR and inserted into the pLJM1 digested with restriction enzymes *AgeI* and *EcoRI* to construct pLJM1-GCaMP6s. A fragment of GFP-LC3 was amplified from the pMRX-IP-GFP-LC3-RFP-LC3ΔG¹⁶ by PCR and inserted into the pLJM1 digested with restriction enzymes *NheI* and *EcoRV* to construct pLJM1-GFP-LC3.

2.4 | Drug screening

The Screen-Well® FDA-approved drug library V2 (BML-2843J Version 1.3) was used for drug screening. A total of 10,000 TGS04 cells were seeded into a 96-well black-wall and clear-bottom plate (Corning) and stained with 60nM LysoTracker™ Red DND-99 (Thermo Fisher Scientific) at 37°C for 30 minutes. Fluorescence intensity was detected before and after treatment with library compounds (0.25, 1.25, and 5 μM) by an X810A (Keyence). The compound efficacy was evaluated by the relative fluorescence intensity.

2.5 | Virus infection and transfection

For lentivirus production, HEK293T cells were cotransfected with a lentiviral vector and packaging vectors (PAX2 and VSVG) at a 1:1:0.5 ratio by X-tremeGENE™ HP (Sigma-Aldrich). For retrovirus production, 293GP cells were cotransfected with a retroviral vector and VSVG at a 1:2.5 ratio by X-tremeGENE™ HP. The medium was changed to NSPC medium at 24 hours post transfection. Supernatant was collected after 48 hours and passed through a 0.45-μm filter. For transduction, GBM cell lines were infected with the lentivirus or retrovirus with 1 μg/ml polybrene (Sigma-Aldrich). TGS04 cells were transfected with 4 μg pLAMP1-mGFP plasmid using an Amaxa mouse neural stem nucleofactor kit (Lonza). HEK293T cells were transfected with 0.5 μg pLAMP1-mCherry and 0.5 μg pLC3-mGFP by using X-tremeGENE™ HP.

2.6 | Sphere-formation assay

Glioblastoma spheroids were dissociated with accutase (STEMCELL Technologies) and washed with NSPC medium. Then, 500 GBM cells or 1000 neural progenitor cells were seeded in NSPC medium containing 1% methylcellulose (Wako) with indicated compounds. GBM spheroids were counted after 10-14 days under a BZ-9000 (Keyence).

2.7 | Immunoblotting

Glioblastoma cells were lysed in RIPA buffer. Equal amounts of proteins were separated by SDS-PAGE and transferred to a PVDF

membrane (Millipore). The membrane was blocked with 5% dry skimmed milk (BD Biosciences) in Tris Buffered Saline with Tween 20 (TBST) and incubated with a primary antibody diluted in Can Get Signal Solution (TOYOBO). Proteins were detected with secondary horseradish peroxidase-conjugated antibodies and ECL prime Western blotting detection reagent (GE Healthcare). Primary antibodies recognizing the following proteins were used: mTOR (catalog no. 2983), phospho-mTOR (S2448) (catalog no. 2971), S6 (catalog no. 2217s), phospho-S6 (Ser235/236) (catalog no. 2211L) (all from Cell Signaling Technologies; 1:1000), LC3 (NanoTools; clone 5F10, 0231; 1:500), SQSTM1 (p62) (Abnova, H00008878-M01; 1:1000), and β-actin (Sigma-Aldrich, A5441; 1:2000).

2.8 | Autophagic flux measurement

The pMRX-IP-GFP-LC3-RFP-LC3ΔG probe was stably expressed in TGS04 cells by retrovirus infection. The cells were treated with 5 μM ifenprodil for 24 hours and then dissociated with accutase. GFP and RFP fluorescence intensities were detected by flow cytometry.

2.9 | Galectin puncta assay

EGFP-hGal3 was stably expressed in GBM cells by lentivirus infection. Then, a 96-well glass bottom microplate (Corning) was coated with 0.1 mg/ml laminin at 37°C for 3 hours and washed with PBS (-) three times. Next, 10,000 GBM cells were seeded onto the plate and incubated at 37°C for 16-24 hours. The cells were treated with DMSO or drugs for 15 minutes and stained with 5 μg/ml Hoechst 33342 (Thermo Fisher Scientific) at 37°C for 15 minutes. Galectin-3-positive puncta were imaged under a ×40 objective water immersion lens by confocal microscopy (Leica).

2.10 | Mitochondrial reactive oxygen species (ROS)

Glioblastoma cells (1×10^5) were treated with DMSO or 5 μM ifenprodil for 6 hours, dissociated with accutase, and washed in PBS (-). Samples were stained with 2.5 μM MitoSox-Red (Thermo Fisher Scientific) for 15 minutes at 37°C, washed in 3% FBS/PBS (-) twice, and then their fluorescence intensity was measured by flow cytometry.

2.11 | Apoptosis

Glioblastoma cells (1×10^5) were treated with DMSO or 5 μM ifenprodil for 6 hours, dissociated, and washed in 3% FBS/PBS (-). The cells were incubated in Annexin V binding buffer (BD Biosciences) containing 5 μl annexin V-FITC (BD Biosciences) and 7-AAD (BD Biosciences) for 15 minutes at room temperature. Fluorescence intensity was measured by flow cytometry.

2.12 | Fluo-4 Ca²⁺ imaging

Thirty thousand GBM cells were seeded on the laminin-coated 48-well plate. After culture for 16–24 hours, the cells were stained with Fluo-4 (Thermo Fisher Scientific) at 37°C for 1 hour. The cells were washed in NSPC medium. KRB calcium-free buffer (Millipore) was used for intracellular calcium detection. Fluorescence intensity was measured every 5 seconds over 10 minutes after drug treatments and analyzed by the BZ-9000.

2.13 | GCaMP6s imaging

GCaMP6s-cytoplasm was stably expressed in GBM cells by lentivirus infection. 30,000 GBM cells were seeded onto the laminin-coated 48-well microplate and incubated at 37°C for 3 hours. The cells were pretreated with 1 mM LLOMe or 10 μM thapsigargin at 37°C for 3 hours. GFP fluorescence intensity was measured after treatment with 2 μM ifenprodil. Images were obtained every 5 seconds over 10 minutes and analyzed by the BZ-9000.

2.14 | Patient-derived xenograft (PDX) model

TGS04 cells (1×10^6) were mixed with NSPC medium and Matrigel (Corning) (1:1 ratio) and subcutaneously transplanted into each of the two flanks of anesthetized female Balb/c nu/nu mice. Transplanted mice were randomly divided into five groups (three mice/group) for drug treatments. Ifenprodil (0.2 and 0.5 mg/kg, daily) was dissolved in DMSO and mixed with corn oil at a 1:4 ratio. CQ (25 mg/kg, daily) was dissolved in PBS (-). All drugs were intraperitoneally (ip) injected into mice for 2 weeks starting on day 1 after transplantation. The width (W) and length (L) of tumors were measured using calipers. The tumor volumes were calculated using the formula: volume = $(W^2 \times L)/2$. For orthotopic PDX, intracranial transplantation was performed on anesthetized 4-week-old female Balb/c nu/nu mice using human patient-derived GBM cells (1×10^5 /mouse). Mice were randomly divided into four groups (five mice/group) for drug treatments: control (DMSO), ifenprodil (5 mg/kg), CQ (50 mg/kg), combination of ifenprodil (5 mg/kg), and CQ (50 mg/kg). Ifenprodil and DMSO were mixed with corn oil at a 1:4 ratio. CQ was dissolved in PBS (-). All drugs were intraperitoneally injected into mice for four cycles (for one cycle, 5 days of injection followed by 2 days of rest) starting on day 1 after transplantation.

2.15 | Statistics

Student's *t* test was used to compare two groups. One-way analysis of variance followed by Tukey's test was used to compare more than two groups. Differences in the survival rate were analyzed by the log-rank test. Significance was calculated using Prism 8 software; **p* < 0.05; ***p* < 0.01; ****p* < 0.001; *****p* < 0.0001.

3 | RESULTS

3.1 | Identification of clinically available compounds to sensitize GBM cells to autophagy inhibition

In previous studies, our screening revealed several compounds that were highly effective to inhibit the growth of ATG5-deficient cells that showed suppression of autophagic activity compared with controls. To identify compounds for clinical application, we focused on FDA-approved compounds, especially those for CNS diseases. It has been reported that dopamine receptor D4 antagonists (PNU 96415E and L-741,742) have an advantage in GBM therapy mediated by modification of autophagy.¹⁷ In the study, ifenprodil was also selected at the final step of screening as a candidate that was effective to suppress the proliferation of GBM cells, but not neural stem cells; however, it has not been well characterized. Ifenprodil is an FDA-approved antagonist of N-methyl-D-aspartate receptors, which is considered to have neuromodulatory activities in psychiatric conditions; therefore, we selected it as a candidate. We found that ifenprodil efficiently inhibited spheroid formation of ATG5-deficient cells (Figure 1A). To examine the therapeutic efficacy of ifenprodil in multiple GBM cell lines, we performed a sphere-formation assay using four different patient-derived GBM cell lines under the same culture conditions. Because the inhibitory effect of ifenprodil was commonly found in several GBM patient samples with high efficacy (IC₅₀: 0.03–1.74 μM) (Figure 1B), we focused on this compound to understand its mechanism. Synergistic effects of ifenprodil with autophagy inhibition were confirmed by pharmacological autophagy inhibitors MRT68921 (ULK inhibitor) and bafilomycin A1 (inhibitor of the vacuolar-type H⁺-ATPase) in multiple GBM cell lines (Figure 1C,D, Figure S1A–D). Although there were variations in the effect of ifenprodil on sphere formation, it was consistently observed that ifenprodil exerted a synergistic effect by inhibition of autophagy under any condition. Treatment with ifenprodil remarkably suppressed the mechanistic target of the rapamycin complex 1 (mTORC1) signaling pathway and increased LC3II/LC3I ratios (Figure 1E), suggesting enhancement of autophagic activity. To confirm these results, we used fluorescent probe GFP-LC3-RFP-LC3ΔG to precisely detect autophagic flux¹⁶ and found that autophagic flux was significantly enhanced by ifenprodil (Figure 1F). Thus, ifenprodil affected mTOR-autophagy pathways and exerted a remarkable synergistic effect on the inhibition of spheroid formation in combination with autophagy inhibition.

3.2 | Cytotoxicity mediated by elevation of intracellular Ca²⁺ level with ifenprodil

Next, we investigated how ifenprodil inhibited spheroid formation of GBM cells. We found that treatment of ifenprodil clearly induced apoptosis in GBM cells (Figure 2A). Because our previous study showed that compounds that induce calcium mobilization synergized with autophagy inhibition to achieve efficient therapy of GBM,¹² we investigated whether ifenprodil affected the intracellular Ca²⁺ level.

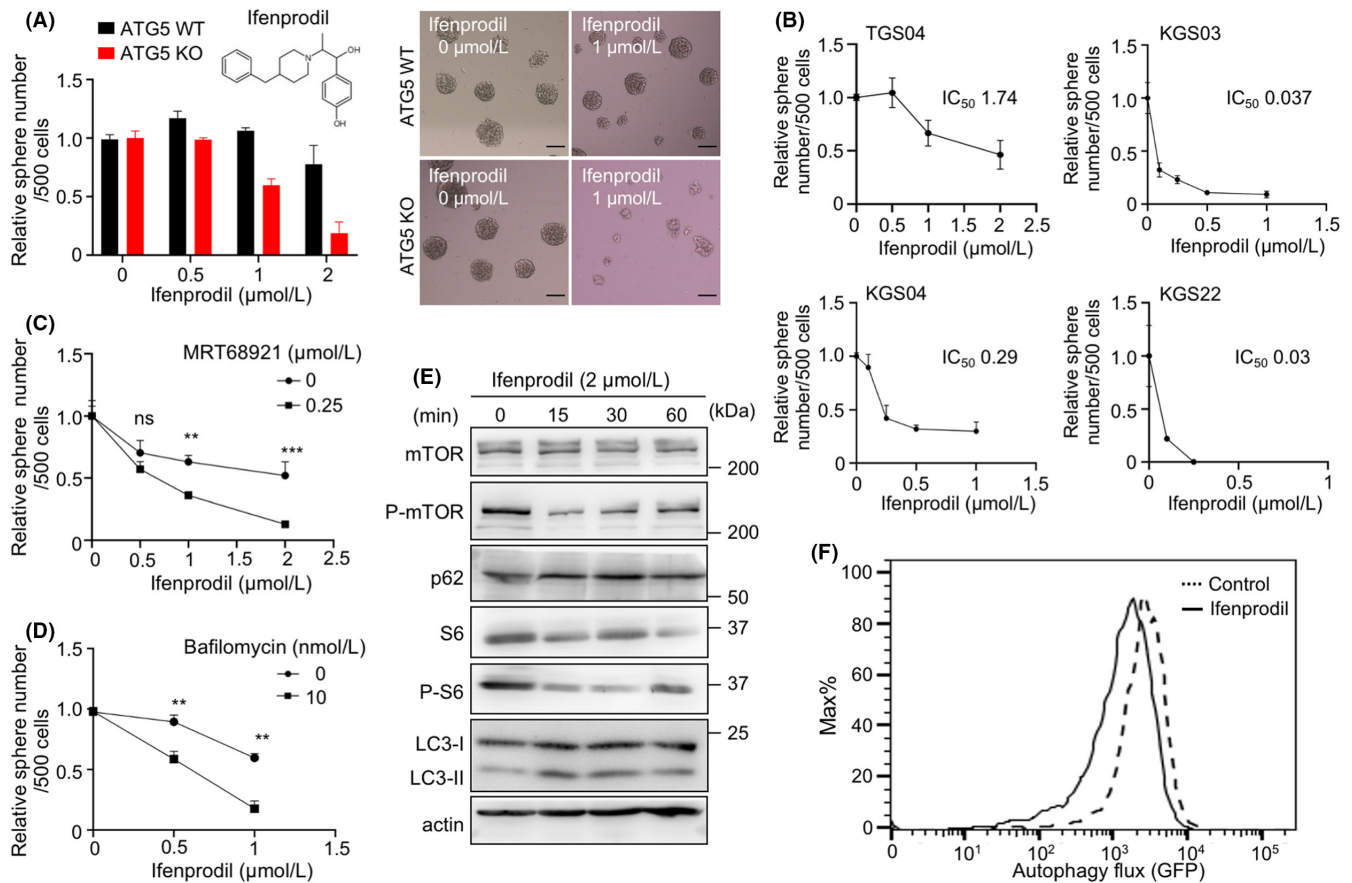


FIGURE 1 Ifenprodil, a clinically available drug, to sensitize glioblastoma (GBM) cells to autophagy inhibition. A, Relative number (left) and representative images of spheroids (right) formed by TGS04 WT and ATG5-KO cells treated with ifenprodil. Data are the mean \pm SD ($n = 3$). Scale bars, 200 μ m. B, Relative number of spheroids formed by TGS04, KGS03, KGS04, and KGS22 cell lines treated with ifenprodil. Data are the mean \pm SD ($n = 3$). The IC₅₀ of ifenprodil in each cell line is indicated. C, Relative number of spheroids formed by TGS04 cells treated with ifenprodil in combination with 0.25 μ M MRT68921. Data are the mean \pm SD ($n = 3$). D, Relative number of spheroids formed by TGS04 cells treated with ifenprodil in combination with 10 nM bafilomycin A1. Data are the mean \pm SD ($n = 3$). E, Western blotting of the indicated proteins in TGS04 cells after treatment with 2 μ M ifenprodil for 15, 30, and 60 min. F, Autophagic flux was detected in TGS04 cells expressing the GFP-LC3-RFP-LC3 Δ G probe after treatment with ifenprodil (black line) or DMSO (dashed black line) for 24 h. Fluorescence intensity of GFP was measured by flow cytometry

Ifenprodil remarkably increased the intracellular Ca²⁺ level measured by the calcium indicator Fluo-4 in GBM cells (Figure 2B). This finding was confirmed by GCaMP, a genetically encoded calcium indicator (Figure 2C, Figure S2A–C). Ca²⁺ chelator BAPTA-AM partially but significantly restored suppression of spheroid formation (Figure 2D), indicating that Ca²⁺ elevation induced by ifenprodil caused cytotoxicity. While mitochondrial ROS were induced by ifenprodil (Figure 2E), treatment with antioxidative reagent, NAC, suppressed this effect (Figure 2F). Thus, ifenprodil increased the intracellular Ca²⁺ level, resulting in cytotoxicity mediated by mitochondrial oxidative stress.

3.3 | A critical role of autophagy in protection against lysosomal membrane damage induced by ifenprodil

Elevation of the intracellular Ca²⁺ level by ifenprodil was found when cells were treated in media without Ca²⁺, and therefore

Ca²⁺ was released from organelles that stored calcium and not from extracellular fluid. Because the ER and lysosomes are major organelles for calcium storage, we treated cells with thapsigargin to deplete calcium storage in the ER by blocking the ability of the cell to pump calcium into the ER, followed by treatment with ifenprodil. We compared the effects of ifenprodil in the presence and absence of thapsigargin pretreatment. There was no difference in the levels of the initial peak between them, indicating that the main response of Ca²⁺ release induced by ifenprodil was not affected by Ca²⁺ storage in the ER (Figure 3A). It was also noted that a rapid reduction of Ca²⁺ levels after ifenprodil stimulation occurred with thapsigargin pretreatment compared with no pretreatment, suggesting that Ca²⁺ storage in the ER affects Ca²⁺ release to a lesser extent because the ER is the main source of Ca²⁺ in lysosomes. In contrast to thapsigargin, ifenprodil-driven calcium elevation was blocked by pretreatment with L-leucyl-L-leucine methyl ester (Figure 3B). Thus, ifenprodil promoted calcium mobilization mainly from lysosomes rather than other organelles. Next, we investigated

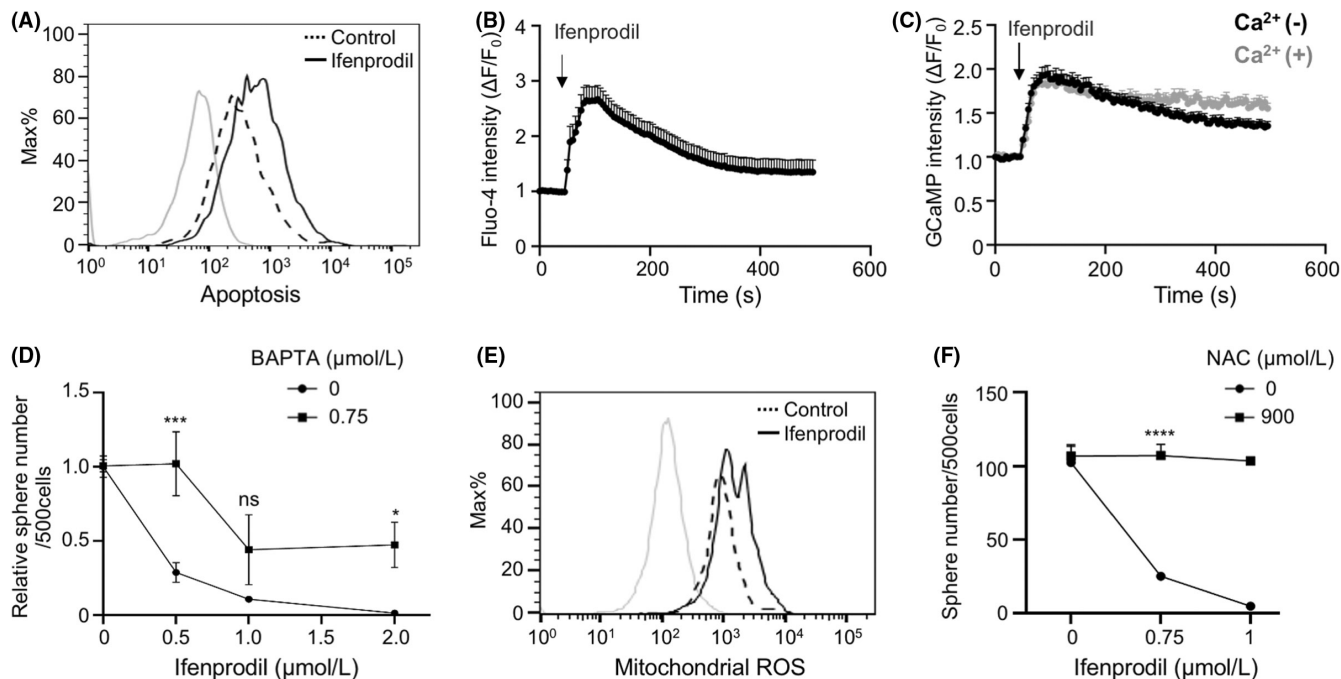


FIGURE 2 Cytotoxicity induced by elevation of intracellular Ca^{2+} level with ifenprodil. A, Flow cytometric analysis of apoptosis by annexin V-FITC staining of TGS04 cells after treatment with 5 μM ifenprodil for 6 h. Gray solid line, unstained control; black dashed line, DMSO control; black solid line, ifenprodil. B, Cytoplasmic calcium dynamics were measured by time lapse imaging in TGS04 cells during treatment with 1 μM ifenprodil by Fluo-4. C, Cytoplasmic calcium dynamics of TGS04 were measured by time lapse imaging in Krebs-Ringer Bicarbonate buffer with or without Ca^{2+} by a GCaMP cytoplasm probe. D, Relative number of spheroids formed by TGS04 cells pretreated with or without 0.75 μM BAPTA for 1 h at 37°C before treatment with ifenprodil. E, Mitochondrial reactive oxygen species (ROS) levels were detected in TGS04 cells for 8 h after treatment with 5 μM ifenprodil by flow cytometry. Gray solid line, unstained control; black dashed line, DMSO control; black solid line, ifenprodil. F, Quantification of the number of spheroids formed by TGS04 cells pretreated with 900 μM N-acetyl-L-cysteine (NAC) for 1 h at 37°C before treatment with ifenprodil

whether autophagy affected Ca^{2+} release from lysosomes induced by ifenprodil. While autophagy inhibition itself did not affect the Ca^{2+} level, it remarkably enhanced the effect of ifenprodil on Ca^{2+} release (Figure 3C). These data suggested that autophagy inhibition enhanced the effects of ifenprodil mediated by modification of lysosomal quality control.

Next, we investigated how ifenprodil induced Ca^{2+} release from lysosomes. Because Ca^{2+} release by ifenprodil occurred rapidly after treatment within several minutes, we assumed that ifenprodil may induce lysosomal membrane rupture because of its chemical properties, like the lysosomotropic agent, LLOMe. To analyze lysosomal membrane damage, we evaluated galectin-3 localization because galectin-3 rapidly translocates to the inner membrane of lysosomes to contribute to clearance or repair of the lysosomal membrane.¹⁸ While galectin-3 localized in cytoplasm without stimulation, ifenprodil treatment induced remarkable puncta formation of galectin-3 after 15 minutes in multiple GBM cell lines, which was similar to LLOMe treatment (Figure 3D, Figure S3B). The result clearly indicated that lysosomal membrane damage was induced by ifenprodil at a much lower concentration (0.5 μM as the minimum dose) than LLOMe (500 μM), indicating that ifenprodil was a potent pharmacological agent that induced lysosomal membrane damage (Figure S3A). While a lower dose

of ifenprodil induced galectin-3 punctation at the minimum level, autophagy inhibition showed remarkable punctation similar to treatment at a higher dose (Figure 3E). These data demonstrated that autophagy protected against lysosomal membrane damage induced by ifenprodil.

3.4 | Screening of compounds that induce lysosomal membrane damage for clinical application

Previous studies have reported the several compounds with the lysosomotropic characteristics, such as LLOMe, CQ, ammonium chloride, methylamine, and siramesine.¹⁹ We hypothesized that FDA-approved drugs may include many compounds that induce lysosomal dysfunction. Therefore, to compare the effectiveness of ifenprodil with that of 765 FDA-approved compounds for induction of lysosome dysfunction, we performed lysotracker staining to determine whether these compounds induced lysosomal dysfunction at various doses (0.25, 1.25, and 5 μM). LLOMe was evaluated as a control at 1 mM. We found that ifenprodil was one of the top 10 compounds at the lower concentrations of 0.25 and 1.25 μM (Figure 4A). Ifenprodil was not the top candidate at the higher concentration, because the higher concentration of

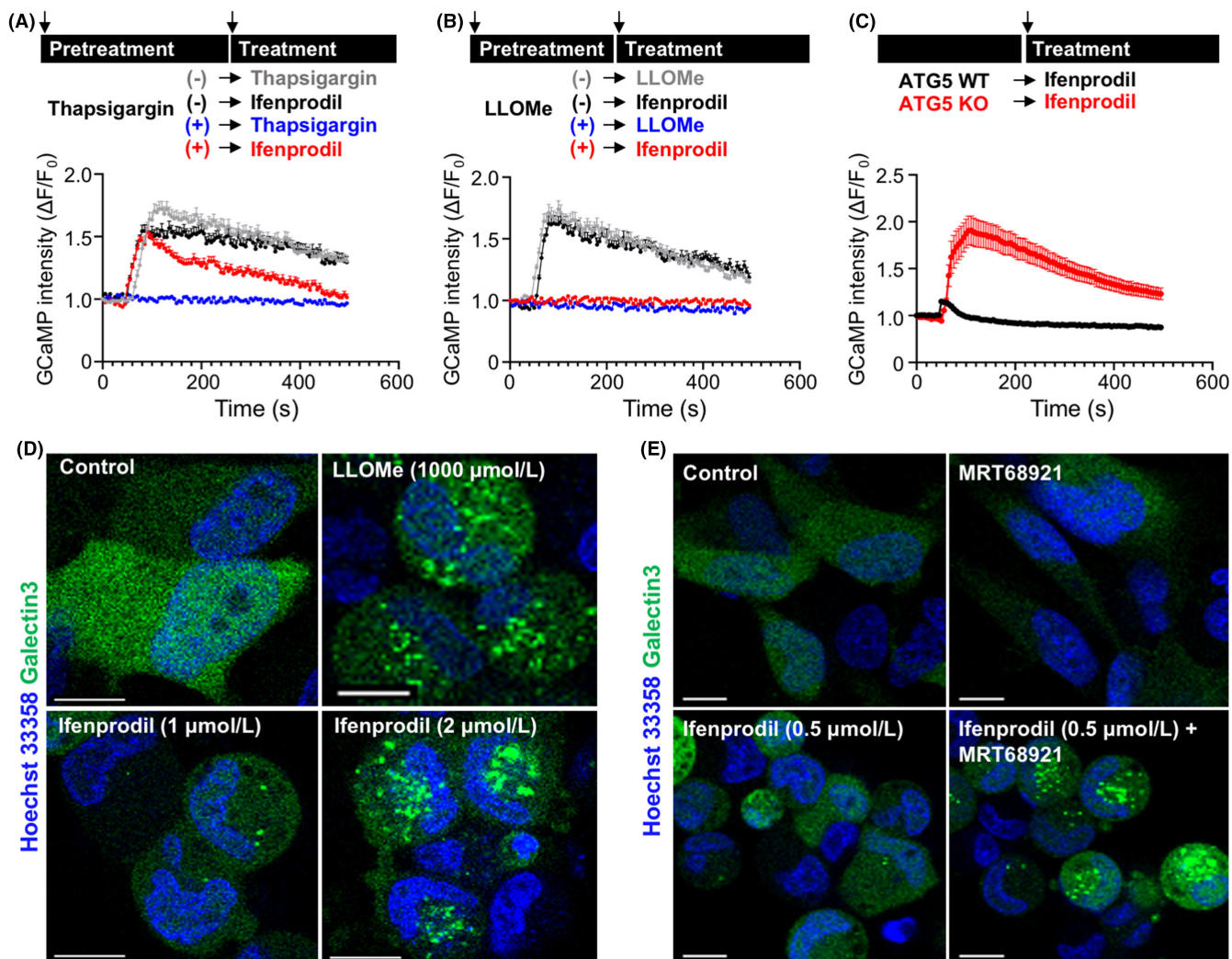


FIGURE 3 Effects of autophagy on lysosomal membrane damage induced by ifenprodil. A, B, Cytoplasmic calcium dynamics were measured by time lapse imaging in TGS04 cells pretreated with 10 μM thapsigargin or 1 mM L-leucyl-L-leucine methyl ester (LLOMe) for 3 h at 37°C before treatment with ifenprodil. C, Cytoplasmic calcium dynamics were measured in TGS04 WT and ATG5-KO cells during treatment with 0.2 μM ifenprodil. D, TGS04 cells expressing GFP-galectin-3 were treated with 1 mM LLOMe or 1 and 2 μM ifenprodil for 15 min. Galectin-3 punctation was observed by microscopy. Scale bars, 10 μm . E, TGS04 cells expressing GFP-galectin-3 were pretreated with 0.25 μM MRT68921 for 16–24 h. Galectin-3 punctation was observed after 15 min of ifenprodil treatment by microscopy. Scale bars, 10 μm

ifenprodil induced cell death (Figure 2A). These results clearly demonstrated an advantage of ifenprodil for clinical application in terms of drug repurposing for lysosomal membrane targeting. Additionally, we found another candidate, amoxapine, for application to GBM patients because it is a tricyclic antidepressant that has been clinically used. In our previous study, we found that amoxapine is a unique compound that exerts remarkable effects on suppression of glioma cells with malignant phenotypes.²⁰ Therefore, we focused on amoxapine among other candidate drugs. We found that amoxapine efficiently induced galectin-3 punctation, enhanced autophagic flux and Ca^{2+} upregulation, and remarkably inhibited spheroid formation of ATG5-deficient cells (Figure 4B–E), suggesting that our strategy was efficient to successfully identify therapeutic reagents that sensitize GBM cells to autophagy inhibitors.

3.5 | Lysosomal membrane turnover driven by compounds

A recent study has demonstrated a selective mechanism of lysosomal membrane degradation that involves lipidation of the autophagy protein LC3 on lysosomal membranes and the formation of intraluminal vesicles through lysophagy as microautophagy,⁷ and therefore we investigated whether lysosomal membrane turnover was stimulated by the compounds. To measure lysosome membrane turnover, cells were treated with ifenprodil after transfection of GFP-tagged lysosomal transmembrane protein LAMP-1 (LAMP1-mGFP). Ifenprodil clearly induced accumulation of untagged GFP protein, as well as LLOMe (Figure 5A), indicating that ifenprodil promoted degradation of lysosomal membrane proteins by cathepsin-mediated digestion in lysosomes. We found that these compounds induced

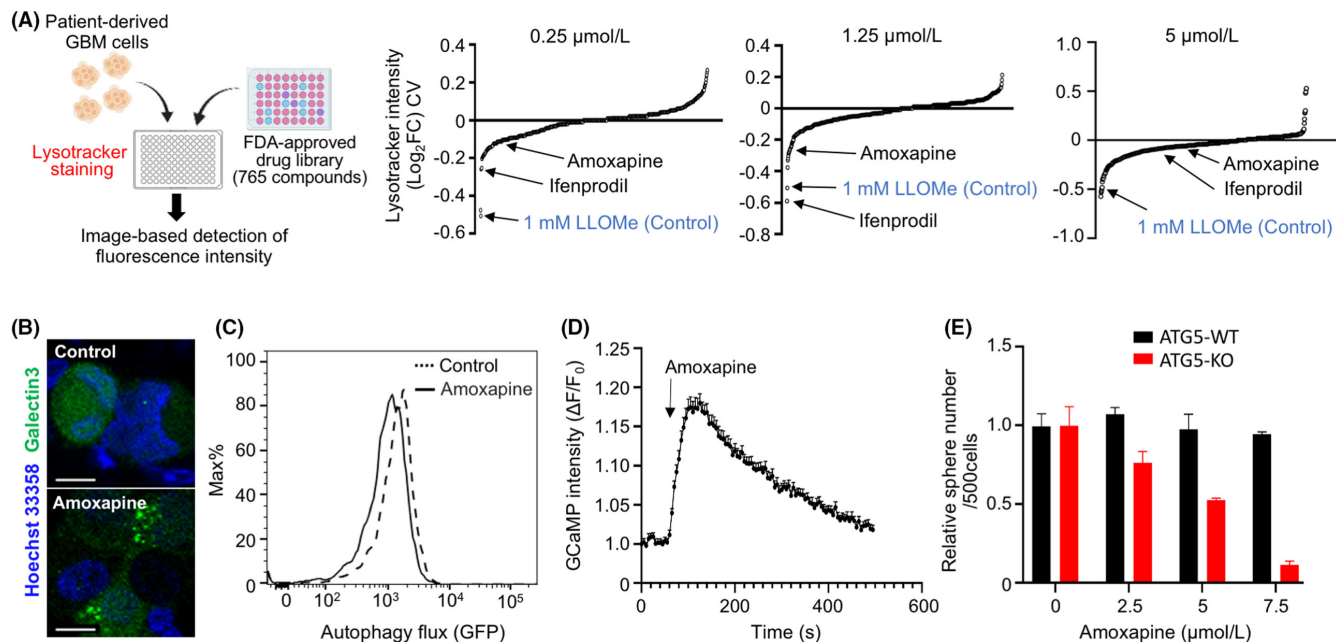


FIGURE 4 Identification of clinically available drugs that induce lysosomal membrane damage for glioblastoma (GBM) therapy. A, Relative fluorescence intensity of lysotracker-red was measured in TGS04 cells treated with 765 library compounds (0.25, 1.25, and 5 μM). L-leucyl-L-leucine methyl ester (LLOMe) (1 mM) was evaluated as a control. B, Galectin-3 punctation was detected in TGS04 cells expressing GFP-galectin-3 after treatment with 10 μM amoxapine for 15 min. C, Autophagic flux was detected in TGS04 cells expressing the GFP-LC3-RFP-LC3 ΔG probe after treatment with 2.5 μM amoxapine (black solid line) or DMSO (black dashed line) for 24 h. D, Cytoplasmic calcium dynamics were measured by time lapse imaging in TGS04 cells during treatment with 2.5 μM amoxapine. E, Relative number of spheroids formed by TGS04 WT and ATG5-KO cells treated with amoxapine

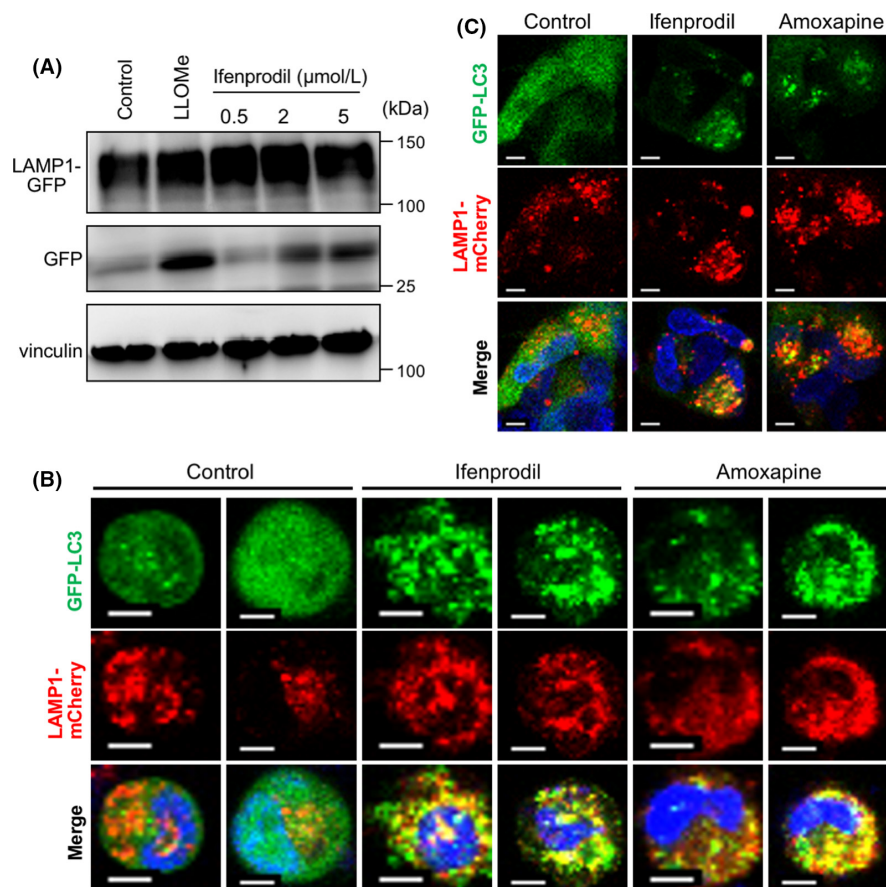


FIGURE 5 Lysosomal membrane turnover induced by compounds. A, Indicated proteins were detected in TGS04 after treatment with 1 mM L-leucyl-L-leucine methyl ester (LLOMe) or 0.5, 2, and 5 μM ifenprodil for 8 h. B, C, Colocalization of LAMP1-mCherry and GFP-LC3 was detected after treatment with 2 μM ifenprodil or 10 μM amoxapine for 2 h in 293T cells (B) and TGS04 cells (C)

LC3 lipidation on the lysosomal membrane (Figure 5B,C). Combined with data of increased lysosomal membrane damage by autophagy inhibition (Figure 3C,E), these data supported an idea that loss of lysophagy contributed to sensitization of GBM cells to compounds that induced lysosomal membrane damage.

3.6 | Therapeutic advantage of triggering lysosomal membrane permeabilization for GBM treatment

Finally, we evaluated whether the compounds were applicable to GBM therapy. Importantly, although ifenprodil was more effective to inhibit spheroid formation when combined with CQ in patient-derived GBM cells (Figure 6A,B), the treatment was not effective in noncancerous, neural progenitor cells derived from human embryos (Figure 6C). We also evaluated the effectiveness of the combination of ifenprodil and CQ in vivo. To this end, we first subcutaneously

transplanted GBM cells into immunocompromised mice and treated them with ifenprodil (0.2 mg/kg) in combination with CQ (25 mg/kg). We found that combinational treatment exhibited a strong inhibitory effect on tumor growth (Figure 6D). No obvious adverse effects due to administration of CQ and ifenprodil were observed during the monitoring period (data not shown). The combinational treatment of amoxapine and CQ also suppressed the tumor growth significantly (Figure S4). Finally, we performed orthotopic PDX by transplantation of GBM cells into the mouse brain. Because preliminary experiments had indicated that the effects of these drugs were not remarkable in orthotopic PDX, unlike subcutaneous PDX, we administrated higher doses (5 mg/kg) of ifenprodil and CQ (50 mg/kg) in this setting. While we did not observe a significant effect of ifenprodil or CQ alone, mouse survival was significantly extended by combinational treatment with CQ and ifenprodil (Figure 6E), suggesting a therapeutic advantage of the combination of these drugs in a clinical setting. These data clearly indicated that targeting lysosomal membrane integrity is a promising target for cancer therapies.

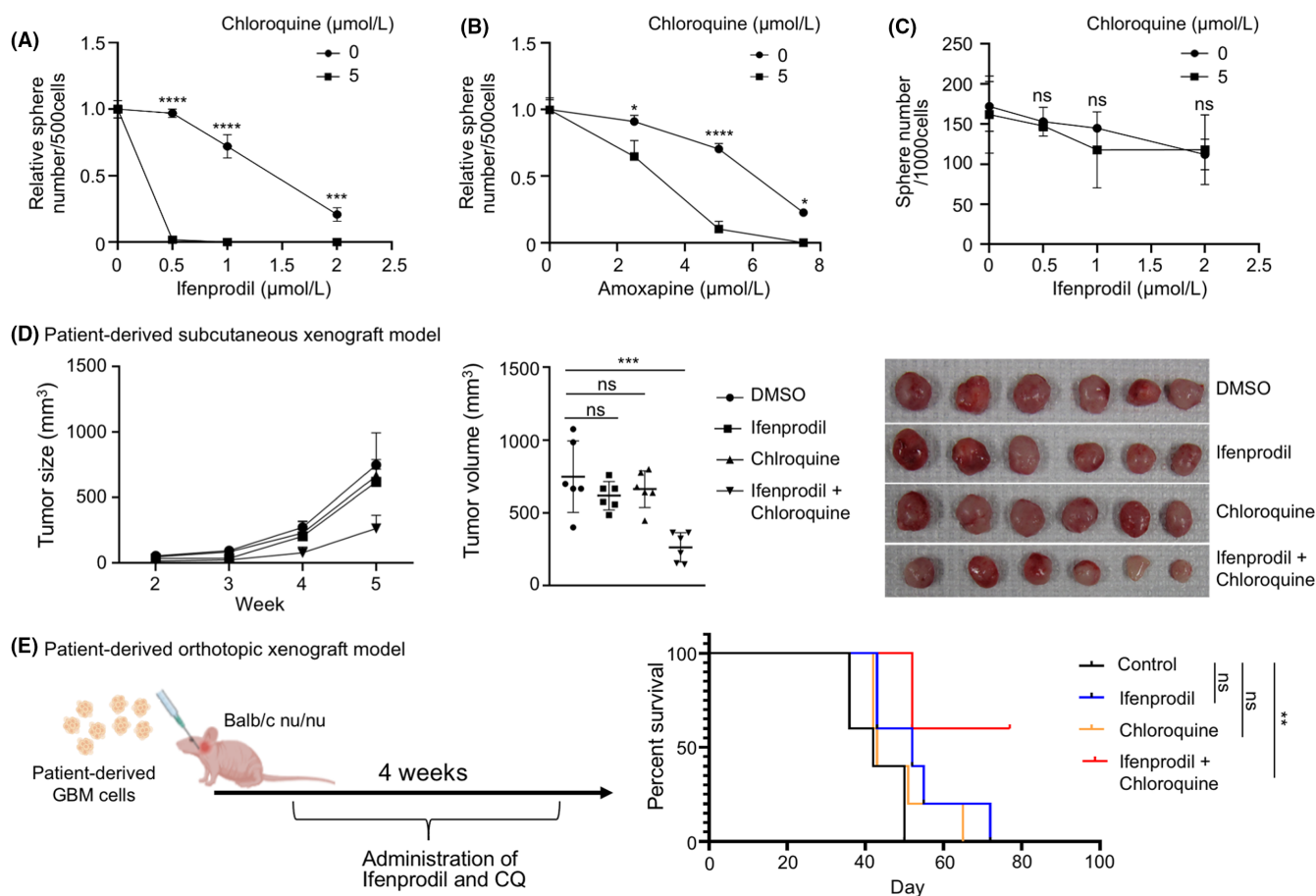


FIGURE 6 Therapeutic advantage of triggering lysosomal membrane permeabilization for glioblastoma (GBM) treatment. A, B, Relative number of spheroids formed by TGS04 cells that were treated with ifenprodil or amoxapine in combination with 5 μM chloroquine (CQ). Data are the mean \pm SD ($n = 3$). C, Relative number of spheroids formed by neural progenitor cells treated with ifenprodil in combination with 5 μM CQ. D, Quantitation of the size (left) and volume (center) of tumors in mice subcutaneously injected with TGS04 cells and treated with DMSO, CQ (ip daily injection of 25 mg/kg), ifenprodil only (ip daily injection of 0.2 mg/kg), or ifenprodil plus CQ. Data are the mean \pm SD. Images of tumors at the experiment endpoint are shown (right) ($n = 6$ /group). E, Kaplan-Meier analysis of survival of recipient mice inoculated in the brain with 1×10^5 TGS04 cells ($n = 5$ mice/group). Mice were treated with DMSO, CQ (i.p. daily injection of 50 mg/kg), ifenprodil only (i.p. daily injection of 5 mg/kg), or ifenprodil plus CQ

4 | DISCUSSION

In this study, by identification of a clinically available drug that induces lysosomal membrane damage, we revealed that quality control of lysosomes by autophagy is a critical therapeutic target. There are two possible mechanisms how the compounds induce autophagy. One is direct stimulation to induce lysosomal membrane turnover as microautophagy (Figure 5A,B). The other one is the induction of macroautophagy by downregulation of mTORC1, presumably due to loss of intact lysosomal membrane (Figure 1E,F). It is assumed that loss of two different autophagy increases sensitivity to compounds targeting lysosomal membrane integrity (Figure 7). We propose a novel concept of a therapeutic advantage by the combination of lysophagy inhibition and pharmacological induction of lysosomal membrane damage for GBM treatment.

The inhibitory effects of CQ and ifenprodil on spheroid formation were remarkable in GBM cells but not in nontransformed neural progenitor cells. These findings indicate that lysosomal activity or functions may be different between normal and malignant cells, and that cancer development and its malignant progression may be highly dependent on lysosomal activity.²¹ For example, lysosomal activity is required to acquire energy essential for cancer cell proliferation.²² Uptake of extracellular materials mediated by phagocytosis, endocytosis, and micropinocytosis is needed to supply carbohydrates, lipids, and amino acids, which support cancer cell proliferation.^{23,24} Thus, the lysosome is a crucial organelle for supplying nutrients.²⁵ When nutrients are rich, mTORC1 is activated on the surface of lysosomes. mTORC1 is one of the most potent promotive factors of cancer cell proliferation, metastasis, and migration.²⁶ Therefore, the lysosome may play a critical role in cancer malignancy. Conversely, when nutrients are lacking, MiT/TFE family transcription factors are

dephosphorylated by inactivation of mTORC1.²⁷ Dephosphorylation of the transcription factors promotes lysosomal functions to supply nutrients.²⁸ Lysosomal calcium also affects cancer cell proliferation and apoptosis.²⁸ Autophagy is involved in the invasion and metastasis of cancer cells. One study has reported that epithelial cell-derived molecules, such as E-cadherin, are degraded by lysosomes, which induces epithelial-mesenchymal transition.²⁹ Modification of the extracellular matrix that controls invasion and metastasis is also regulated by lysosomal degradation.³⁰ Additionally, lysosome activity is involved in angiogenesis and immunity,³¹ which characterize cancer-specific cell behaviors. Thus, it is assumed that the cancer-specific lysosomal regulation manner leads to cell death induced by targeting lysosomal membrane integrity.

While there is no information on the efficiency of penetration across the BBB regarding bafilomycin and MRT68921, CQ is clinically available and data on CQ have been reported in several studies. A study reported that CQ crosses the BBB easily and potentially accumulates in the brain,³² whereas another study indicated that the ability of CQ to cross the BBB is quite limited.³³ Therefore, this issue is controversial. Several clinical trials of CQ have been conducted for various cancers, but the results have not been encouraging.^{11,34} For example, a phase I/II trial that used CQ in combination with chemotherapy and radiation therapy found no significant improvement in the survival of GBM patients.¹¹ The reason for the poor results may be insufficient inhibition of autophagy due to dose-limiting toxicities such as myelosuppression. Thus, it is likely that therapy with CQ appears to be insufficient for lysosomal dysfunction in cancer therapy.³⁵ Therefore, our proposal to combine lysosomal targeting drugs with autophagy inhibitors may be a reasonable solution. As a result, we found that the combination therapy significantly prolonged survival. It is unclear whether CQ and/or ifenprodil cross the BBB because there is the possibility that the effectiveness of CQ may be due to disruption of the BBB by brain tumors. However, in any case, our data support that the combination of these drugs may lead to a favorable outcome in a clinical setting. Further characterization of compounds that target lysosome biogenesis may lead to successful cancer therapy in the future.

ACKNOWLEDGMENTS

We thank Dr Noboru Mizushima for the GFP-LC3-RFP-LC3ΔG probe, Dr Esteban Dell'Angelica for LAMP1-mGFP, Dr Michael Davidson for mCherry-Lysosomes-20, Dr Tamotsu Yoshimori for pEGFP-hGal3, and Dr Douglas Kim & GENIE Project for pGP-CMV-GCaMP6s. We thank Kazue Sawa and Yukiko Takai for expert technical support. We thank Cancer Research Institute, Kanazawa University for the FDA approved drug library Japan version (ENZO; CB-BML2841J0100). We also thank Mitchell Arico from Edanz (<https://jp.edanz.com/ac>) for editing a draft of this manuscript.

DISCLOSURE

Tomoki Todo, Mitsutoshi Nakada, and Atsushi Hirao are the editorial board members of Cancer Science. Other authors have no conflict of interest.

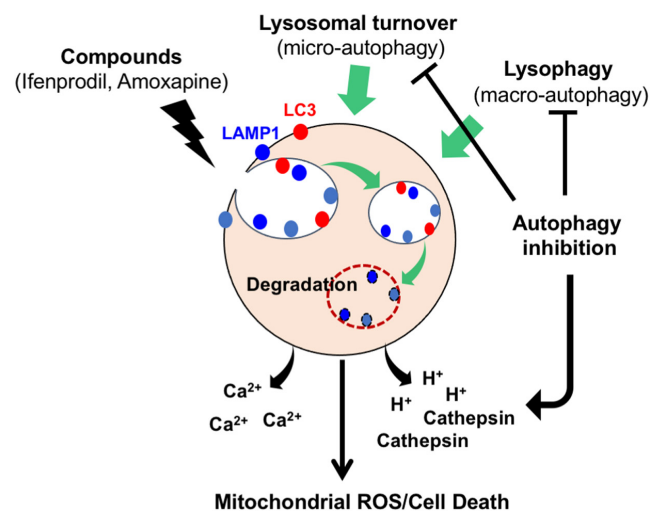


FIGURE 7 Illustration showing the mechanisms of synergistic effects of compounds that induce lysosomal membrane damage and autophagy inhibition. Loss of the protective functions of micro- and macroautophagy sensitizes glioblastoma (GBM) cells to compounds, such as ifenprodil and amoxapine, resulting in cell death mediated by mitochondrial oxidative stress

ETHICS STATEMENT

Collection of human materials and related experimental protocols were approved by the Ethics Committees of Kanazawa University and The University of Tokyo. All animal experiments were approved by the Committee on Animal Experimentation of Kanazawa University and performed following the university's guidelines for the care and use of laboratory animals.

ORCID

Mitsutoshi Nakada  <https://orcid.org/0000-0001-9419-6101>

Atsushi Hirao  <https://orcid.org/0000-0001-7818-8240>

REFERENCES

- Levy JMM, Towers CG, Thorburn A. Targeting autophagy in cancer. *Nat Rev Cancer*. 2017;17:528-542.
- Yun HR, Jo YH, Kim J, Shin Y, Kim SS, Choi TG. Roles of autophagy in oxidative stress. *Int J Mol Sci*. 2020;21:3189.
- Kim KH, Lee MS. Autophagy--a key player in cellular and body metabolism. *Nat Rev Endocrinol*. 2014;10:322-337.
- Hosokawa N, Hara T, Kaizuka T, et al. Nutrient-dependent mTORC1 association with the ULK1-Atg13-FIP200 complex required for autophagy. *Mol Biol Cell*. 2009;20:1981-1991.
- Zientara-Rytter K, Subramani S. Mechanistic insights into the role of Atg11 in selective autophagy. *J Mol Biol*. 2020;432:104-122.
- Kravic B, Behrends C, Meyer H. Regulation of lysosome integrity and lysophagy by the ubiquitin-conjugating enzyme UBE2QL1. *Autophagy*. 2020;16:179-180.
- Lee C, Lamech L, Johns E, Overholtzer M. Selective lysosome membrane turnover is induced by nutrient starvation. *Dev Cell*. 2020;55:289-297. e284.
- Chen R, Smith-Cohn M, Cohen AL, Colman H. Glioma subclassifications and their clinical significance. *Neurotherapeutics*. 2017;14:284-297.
- Ostrom QT, Bauchet L, Davis FG, et al. The epidemiology of glioma in adults: a "state of the science" review. *Neuro Oncol*. 2014;16:896-913.
- Shchors K, Massaras A, Hanahan D. Dual targeting of the autophagic regulatory circuitry in gliomas with repurposed drugs elicits cell-lethal autophagy and therapeutic benefit. *Cancer Cell*. 2015;28:456-471.
- Rosenfeld MR, Ye X, Supko JG, et al. A phase I/II trial of hydroxychloroquine in conjunction with radiation therapy and concurrent and adjuvant temozolomide in patients with newly diagnosed glioblastoma multiforme. *Autophagy*. 2014;10:1359-1368.
- Vu HT, Kobayashi M, Hegazy AM, et al. Autophagy inhibition synergizes with calcium mobilization to achieve efficient therapy of malignant gliomas. *Cancer Sci*. 2018;109:2497-2508.
- Falcón-Pérez JM, Nazarian R, Sabatti C, Dell'Angelica EC. Distribution and dynamics of Lamp1-containing endocytic organelles in fibroblasts deficient in BLOC-3. *J Cell Sci*. 2005;118:5243-5255.
- Maejima I, Takahashi A, Omori H, et al. Autophagy sequesters damaged lysosomes to control lysosomal biogenesis and kidney injury. *EMBO J*. 2013;32:2336-2347.
- Chen TW, Wardill TJ, Sun Y, et al. Ultrasensitive fluorescent proteins for imaging neuronal activity. *Nature*. 2013;499:295-300.
- Kaizuka T, Morishita H, Hama Y, et al. An autophagic flux probe that releases an internal control. *Mol Cell*. 2016;64:835-849.
- Dolma S, Selvadurai HJ, Lan X, et al. Inhibition of dopamine receptor D4 impedes autophagic flux, proliferation, and survival of glioblastoma stem cells. *Cancer Cell*. 2016;29:859-873.
- Aits S, Krickler J, Liu B, et al. Sensitive detection of lysosomal membrane permeabilization by lysosomal galectin puncta assay. *Autophagy*. 2015;11:1408-1424.
- Decker RS, Decker ML, Thomas V, Fuseler JW. Responses of cultured cardiac myocytes to lysosomotropic compounds and methylated amino acids. *J Cell Sci*. 1985;74:119-135.
- Hegazy AM, Yamada D, Kobayashi M, et al. Therapeutic strategy for targeting aggressive malignant gliomas by disrupting their energy balance. *J Biol Chem*. 2016;291:21496-21509.
- Zhu X, Zhuo Y, Wu S, et al. TFEB promotes prostate cancer progression via regulating ABCA2-dependent lysosomal biogenesis. *Front Oncol*. 2021;11:632524.
- Brisson L, Bański P, Sboarina M, et al. Lactate dehydrogenase B controls lysosome activity and autophagy in cancer. *Cancer Cell*. 2016;30:418-431.
- Shao X, Cao G, Chen D, et al. Placental trophoblast syncytialization potentiates macropinocytosis via mTOR signaling to adapt to reduced amino acid supply. *Proc Natl Acad Sci USA*. 2021;118:e2017092118.
- Tang T, Yang ZY, Wang D, et al. The role of lysosomes in cancer development and progression. *Cell Biosci*. 2020;10:131.
- Lawrence RE, Zoncu R. The lysosome as a cellular Centre for signalling, metabolism and quality control. *Nat Cell Biol*. 2019;21:133-142.
- DeBerardinis RJ, Lum JJ, Hatzivassiliou G, Thompson CB. The biology of cancer: metabolic reprogramming fuels cell growth and proliferation. *Cell Metab*. 2008;7:11-20.
- Napolitano G, Esposito A, Choi H, et al. mTOR-dependent phosphorylation controls TFEB nuclear export. *Nat Commun*. 2018;9:3312.
- Settembre C, Zoncu R, Medina DL, et al. A lysosome-to-nucleus signalling mechanism senses and regulates the lysosome via mTOR and TFEB. *EMBO J*. 2012;31:1095-1108.
- Sun T, Jiao L, Wang Y, Yu Y, Ming L. SIRT1 induces epithelial-mesenchymal transition by promoting autophagic degradation of E-cadherin in melanoma cells. *Cell Death Dis*. 2018;9:136.
- Shojima K, Sato A, Hanaki H, et al. Wnt5a promotes cancer cell invasion and proliferation by receptor-mediated endocytosis-dependent and -independent mechanisms, respectively. *Sci Rep*. 2015;5:8042.
- Zhao Q, Gong Z, Li Z, et al. Target reprogramming lysosomes of CD8+ T cells by a mineralized metal-organic framework for cancer immunotherapy. *Adv Mater*. 2021;33:e2100616.
- Compter I, Eekers DBP, Hoeben A, et al. Chloroquine combined with concurrent radiotherapy and temozolomide for newly diagnosed glioblastoma: a phase IB trial. *Autophagy*. 2021;17:2604-2612.
- Xu H, Zhang XY, Wang WW, Wang J. Hydroxychloroquine increased anxiety-like behaviors and disrupted the expression of some related genes in the mouse brain. *Front Pharmacol*. 2021;12:633112.
- Rojas-Puentes LL, Gonzalez-Pinedo M, Crismatt A, et al. Phase II randomized, double-blind, placebo-controlled study of whole-brain irradiation with concomitant chloroquine for brain metastases. *Radiat Oncol*. 2013;8:209.
- Maes H, Kuchnio A, Peric A, et al. Tumor vessel normalization by chloroquine independent of autophagy. *Cancer Cell*. 2014;26:190-206.

SUPPORTING INFORMATION

Additional supporting information may be found in the online version of the article at the publisher's website.

How to cite this article: Jing Y, Kobayashi M, Vu HT, et al. Therapeutic advantage of targeting lysosomal membrane integrity supported by lysophagy in malignant glioma. *Cancer Sci*. 2022;113:2716-2726. doi: [10.1111/cas.15451](https://doi.org/10.1111/cas.15451)